Adaptive Equalization for Filter Bank Based Multicarrier Systems

Dirk S. Waldhauser, Leonardo G. Baltar and Josef A. Nossek
Technische Universität München
Institute for Circuit Theory and Signal Processing
Arcisstr. 21, 80290 München, Germany
Email: {waldhauser, leo.baltar, josef.a.nossek}@tum.de

***Abstract*— Filter bank based multicarrier systems (FBMC) offer a number of benefits over conventional orthogonal frequency division multiplexing (OFDM) with cyclic prefix (CP). One benefit is the improved spectral efficiency by not using a redundant CP and by having much better control of out-of-band emission. Another advantage is the ease of accomodating multiple users in an FDMA fashion especially in the uplink, i. e. the multiple access channel (MAC). On the other hand, more elaborate equalization concepts are needed compared to the single-tap per-subcarrier equalizer sufficient in the OFDM with CP case.**

Therefore, we will present a least-mean-square (LMS) algorithm which is adapted to the principle of orthogonally multiplexed QAM filter banks (OQAM-FBMC). This leads to an adaptive equalizer solution with low complexity. The initialization of the LMS equalizer results from a pilot based channel estimation. The results will be compared with a classical OFDM system, where the loss in data rate is compensated with a higher modulation scheme.

I. Introduction

Multicarrier systems provide many attractive properties for high rate wireless and wireline communication systems [1], [2]. Therefore, many current standards like HIPERLAN/2 [3], IEEE 802.11x (WiFi), IEEE 802.16 (WiMAX), DVB and xDSL use multicarrier modulation. Moreover, multicarrier systems are very prominent candidates for the next generation of mobile communication systems. The mentioned standards are based on OFDM with CP which provides on the one hand a simple equalization as long as the CP covers the impulse response of the channel. On the other hand this CP decreases the bandwidth efficiency of the system because of the transmitted redundancy and the considerable levels of out-of-band radiation [4]. The equalizers would be very complex without the use of the CP because the poor stopband attenuation of the subchannel filters (DFT, IDFT) would lead to a significant overlap between all subchannels.

Several research activities in the last decade suggest to return to the original idea from the late 1960's [5] and use OQAM-FBMCs with subchannel filters which only overlap with directly adjacent subchannels and abandon the CP. This leads to bandwidth efficient systems which necessitate an equalizer in a frequency selective fading environment. We refrain from using subchannel filters with perfect reconstruction because the channel destroys this property anyway. We use truncated square root raised cosine (RRC) FIR filters instead.

The authors of [6], [7] have given a very efficient implementation of OQAM-FBMCs by the use of the polyphase decomposition, also known as Modified DFT filter banks (MDFT) [8].

The main problem up to now is the design and complexity of the equalizers for these systems. In [1] and the references therein some solutions for the channel equalization in FBMC systems are given. Most of them are not satisfactory in the sense that they either aim at equalizing the frequency response of the subchannel, work at the symbol rate or use adjacent subchannels [9]. Equalizing the frequency response does not allow for a direct control of the residual interference in the output signal. Working at the symbol rate suffers from irrevocable aliasing in the signal whereas utilizing adjacent subchannels elevates the complexity.

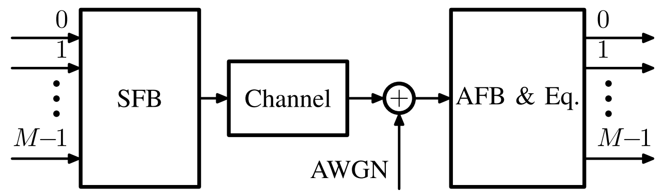

Fig. 1. FBMC System Overview

In this work we use the LMS algorithm as adaptive equalizer solution aiming at the minimum mean-square error (MMSE). In the following we adapt the LMS algorithm of QAM systems to the OQAM characteristics of the filter bank. We use a per-subchannel equalizer which works at $T/2$, where T is the symbol duration. The initial value of the LMS equalizer is obtained by a pilot based channel estimation technique used in CP-OFDM systems. Instead of using improved versions of the family of LMS filters we restrict our analysis to the simple LMS algorithm because we would like to provide a fundamental approach which can easily be extended for specific requirements, keep the complexity of the algorithm low and show that even this simple solution leads to remarkable results. We compare the simulation results with a CP-OFDM system providing the same data rate in a typical HIPERLAN/2 [3] scenario.

A. Notation

For convenience we will use the following notation in the subsequent part of the paper. The real and imaginary part of a signal, an impulse response or any matrix are written as $\mathrm{Re}[(\bullet)] = (\bullet)^{(\mathrm{R})}$ and $\mathrm{Im}[(\bullet)] = (\bullet)^{(\mathrm{I})}$, which means that $(\bullet) = (\bullet)^{(\mathrm{R})} + \mathrm{j}\,(\bullet)^{(\mathrm{I})}$, with $\mathrm{j} = \sqrt{-1}$. Vectors with a time index like $\boldsymbol{x}[n]$ are always compact notations for the $(N+1)$-dimensional vector $\left[x[n], x[n-1], \ldots, x[n-N]\right]^{\mathrm{T}}$, where N is explicitly given each time.

II. Structure of the FBMC System

The structure of the FBMC system is depicted in Fig. 1. The synthesis filter bank (SFB) combines the M low rate subchannel signals into one high rate signal which is transmitted over a frequency selective radio channel. Additive white Gaussian noise (AWGN) is added at the receiver input. The receiver consists of an analysis filter bank (AFB) which splits the received high rate signal into M low rate subchannel signals again. One FIR equalizer per subchannel is employed to compensate for the intersymbol (ISI) and interchannel interference (ICI) caused by the frequency selective radio channel and improve the symbol decisions.

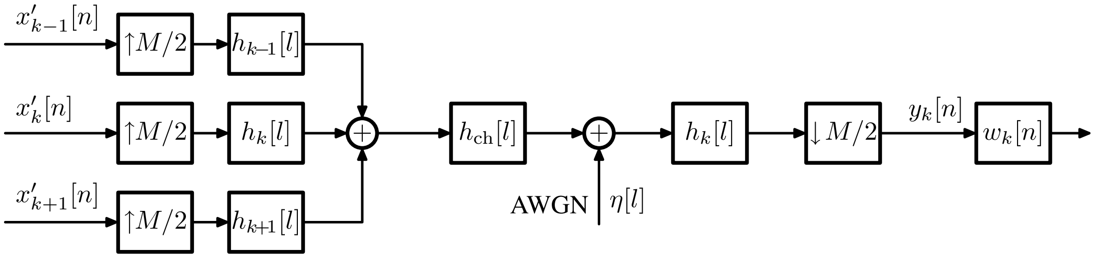

Fig. 2. Subchannel Model for the FBMC System

It is known from the theory of filter banks and transmultiplexers that prototype filters of exponentially modulated filter banks whose length exceeds the number of subchannels have to be implemented in an orthogonally staggered way which leads to orthogonally multiplexed QAM filter banks [5]. We will restrict the derivations of this work to such OQAM filter banks. Details of the SFB and AFB block with equalization are given in the next section but without displaying the efficient implementation [7] for the sake of clarity.

III. Adaptive Channel Equalization

The complexity of the equalizer which is derived in this paper is limited by the fact that only directly adjacent subbands show significant overlap. We only use a single but $T/2$-spaced equalizer for each subband k of the M subbands (cf. Fig. 2), which are obtained by the exponential modulation of a zero-phase prototype filter $h_0[l]$ with length $KM+1$ according to

$$h_k[l] = h_0[l]\exp\left(\mathrm{j}\,2\pi kl/M\right), \quad l=-KM/2,\ldots,KM/2. \quad (1)$$

Therefore, the equalizer is able to remove the distortion before aliasing of the spectral components occurs and allows for restoring the orthogonality of the subcarriers without considering the received symbols of adjacent carriers.

The conventional LMS algorithm [10] has to be adapted to the orthogonal multiplexing of the subchannels. After equalizing the received subchannel signal $y_k[n]$ with the LMS controlled FIR filter $w_k[n]$ we get the following two equations for the estimation of the real and imaginary part of the input symbol according to Fig. 3

$$\begin{aligned}\mathrm{Re}\left[\boldsymbol{w}_k^{\mathrm{H}}\boldsymbol{y}_k[n]\right] &= \boldsymbol{w}_k^{(\mathrm{R}),\mathrm{T}}\boldsymbol{y}_k^{(\mathrm{R})}[n] + \boldsymbol{w}_k^{(\mathrm{I}),\mathrm{T}}\boldsymbol{y}_k^{(\mathrm{I})}[n] \\ &= \hat{a}_k[m], \quad n=2m, \quad m\in\mathbb{Z},\end{aligned} \quad (2)$$

$$\begin{aligned}\mathrm{Im}\left[\boldsymbol{w}_k^{\mathrm{H}}\boldsymbol{y}_k[n-1]\right] &= \boldsymbol{w}_k^{(\mathrm{R}),\mathrm{T}}\boldsymbol{y}_k^{(\mathrm{I})}[n-1] - \boldsymbol{w}_k^{(\mathrm{I}),\mathrm{T}}\boldsymbol{y}_k^{(\mathrm{R})}[n-1] \\ &= \hat{b}_k[m], \quad n=2m, \quad m\in\mathbb{Z},\end{aligned} \quad (3)$$

where $\boldsymbol{w}_k$ and $\boldsymbol{y}_k[n]$ are $\mathbb{C}^N$ vectors, i. e. N corresponds to the number of equalizer coefficients. $\hat{d}_k[m] = \hat{a}_k[m] + \mathrm{j}\,\hat{b}_k[m]$ is an estimation for the transmitted symbol $d_k[m]$ of Fig. 4.

It is also important to mention that the OQAM structure necessitates that the real and imaginary part of Figs. 3 and 4 are interchanged from subchannel to subchannel.

We use the same filter vector $\boldsymbol{w}_k$ in (2) and (3) because it is optimum for both the real and imaginary part of $\hat{d}_k[m]$ under the assumption of additive white Gaussian noise and uncorrelated input symbols.

For updating the filter vector $\boldsymbol{w}_k$ we have to determine the error signal $\epsilon_k[m]$ in Fig. 5 by

$$\epsilon_k[m] = \tilde{d}_k[m] - \hat{d}_k[m] = \mathrm{Q}(\hat{d}_k[m]) - \hat{d}_k[m], \quad (4)$$

where $\mathrm{Q}(\hat{d}_k[m])$ determines the nearest symbol of the corresponding modulation alphabet from $\hat{d}_k[m]$ by a hard decision.

Therefore, we are able to update the filter vector every half symbol duration with either a pure real or a pure imaginary error signal. The error signal $e_k[n]$ for the update process of the $T/2$ spaced filter vector results to

$$e_k[n] = \begin{cases} \epsilon_k^{(\mathrm{R})}[n/2], & n=2m, \quad m\in\mathbb{Z}, \\ \mathrm{j}\,\epsilon_k^{(\mathrm{I})}[(n-1)/2], & n=2m+1, \quad m\in\mathbb{Z}, \end{cases} \quad (5)$$

where the role of real and imaginary parts is interchanged again from subchannel to subchannel. In the QAM case we would update only every symbol duration T but with complex instead of pure real or pure imaginary values.

The LMS adaptation is operated in the decision directed mode because the error is calculated based on the decisions of the estimated symbols $\hat{d}_k[m]$. It is clear that either a good initial value $\boldsymbol{w}_k[0]$ for the equalizer has to be provided or pilot symbols have to be sent. Otherwise the decision of the symbols would be very unreliable and no convergence of the stochastic gradient based LMS algorithm would be achieved.

In Section IV we will show how reasonable initial values $\boldsymbol{w}_k[0]$ are yielded by pilot based channel estimation, which allow for an operation in the decision directed mode.

The tap weight adaption for the equalizer uses the error signal from (5) in the following way (cf. Fig. 5)

$$\boldsymbol{w}_k[n+1] = \boldsymbol{w}_k[n] + \Delta\boldsymbol{w}_k[n] = \boldsymbol{w}_k[n] + \mu\boldsymbol{y}_k[n]e_k^*[n], \quad (6)$$

where μ is the step-size parameter of the LMS algorithm. According to the literature [10] we have chosen the step-size parameter to

$$\mu = \frac{0.2}{\mathrm{tr}\,\boldsymbol{R}_{y_k}}, \quad (7)$$

which corresponds to a misadjustment of $10\,\%$.

We estimate the correlation matrix $\boldsymbol{R}_{y_k}$ of the equalizer input signal $y_k[n]$ by taking the sample mean of the instantaneous correlation matrices

$$\boldsymbol{R}_{y_k} = \frac{1}{2B}\sum_{n=0}^{2B-1}\boldsymbol{y}_k[n]\boldsymbol{y}_k^{\mathrm{H}}[n], \quad (8)$$

where B is number of data symbols in the block between the repeated pilot symbols.

It is worth mentioning that this modified LMS algorithm can also be applied to single carrier systems with OQAM modulation.

IV. Pilot based Channel Estimation

We will use a pilot based channel estimation approach which is already known from the OFDM literature [11]. The HIPERLAN/2 standard [3] specifies two pilot symbols which are spread over all used subcarrriers in the preamble of each burst. The approach uses

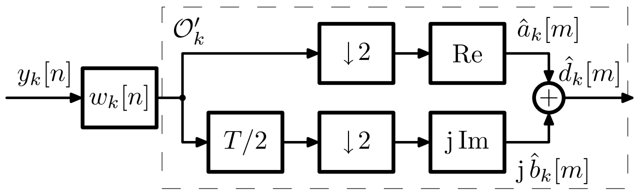

Fig. 3. OQAM De-Staggering $\mathcal{O}'_k$

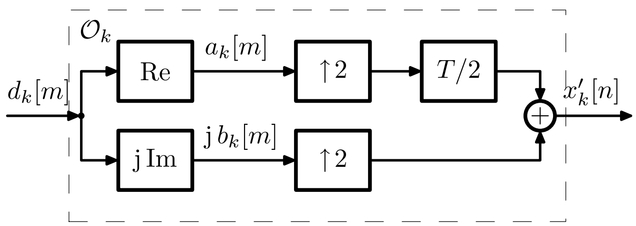

Fig. 4. OQAM Staggering $\mathcal{O}_k$

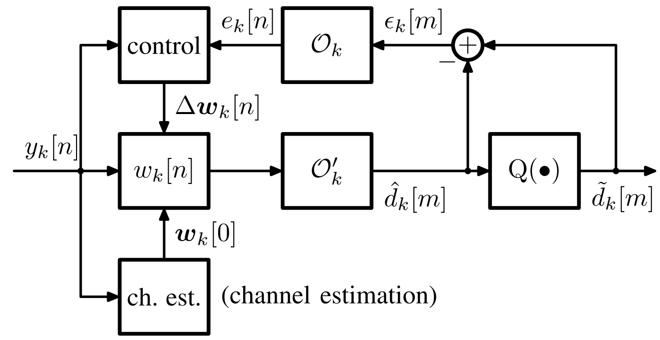

Fig. 5. OQAM-LMS (Decision Directed Mode)

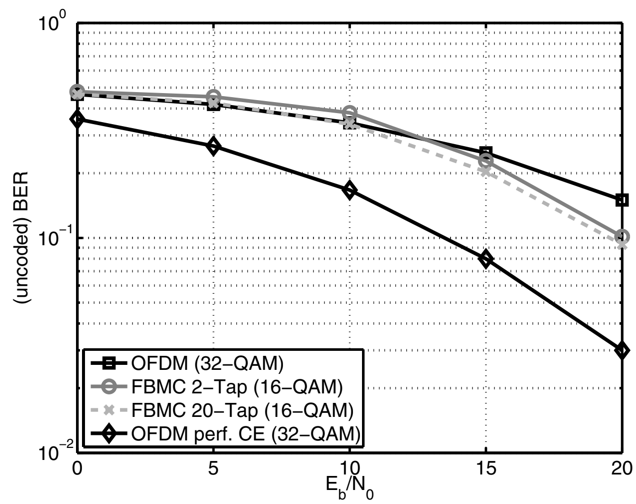

Fig. 6. Comparison of FBMC with CP-OFDM (Modulation Adjusted Such that Both Systems Offer the Same Throughput in Spite of CP)

the knowledge about the standardized pilot sequence and the zeroed subcarriers in order to calculate the noise-reduced channel estimation. The CP-OFDM system uses the estimated subchannel coefficients for one-tap MMSE channel equalization whereas the FBMC system uses these coefficients for calculating the only nonzero entry of the initial MMSE equalizer vectors $\boldsymbol{w}_k[0]$. Since the OFDM system and the FBMC system get the same channel estimates, this approach leads to a fair comparison. On the other hand the flexibility of the FBMC approach allows for using this pilot based channel estimation in the case of HIPERLAN/2, because we can very easily omit the filter operation of the subchannel filters and add a cyclic prefix to the pilots. In this case, we only get better use of spectral efficiency in the payload phase and the out-of-band radiation is increased relative to the amount of pilot symbols to payload data. In practical cases this will be negligible because the pilot phase should be small compared to the payload phase.

It is certainly possible and reasonable to derive a channel estimation for the FBMC system without switching to the OFDM channel estimation mode.

V. Simulation Results

We use a typical HIPERLAN/2 [3] setup in the simulation of our FBMC system with equalizer and an OFDM system with CP. The number of subcarriers is $M = 64$, where $M_\mathrm{t} = 52$ are used for data and pilot transmission. The DC carrier and 11 carriers at both edges of the transmit power spectrum are zeroed out. The CP length is $M_\mathrm{cp} = 16$, which means that 20% of the bandwidth efficiency is sacrified for the CP transmission. In order to provide both systems with the same data rate, we compensate the CP loss of OFDM by adapting different fixed modulation alphabets for both systems. Therefore, we use 16-QAM for the FBMC and 32-QAM for OFDM. Although the HIPERLAN/2 spectrum mask, which is adapted to OFDM, would even allow the use of 4 further subcarriers of the FBMC system, we neglect this fact in our comparison.

We use the power delay profile "Model B" from the channel model specification [12] of HIPERLAN/2, which possesses 16 coefficients and fits to the CP length. We average about many channel realizations, which are constant during each burst. The bursts consist of 2 pilot symbols in the preamble, which allow for the channel estimation, and a payload block of $B = 2000$ symbols.

The prototype filter $h_0[l]$ is specified as RRC FIR filter with a roll-off factor $\rho = 0.5$ and 257 coefficients (overlapping factor $K = 4$). The length of the FBMC equalizer in the AFB is chosen to 2 and 20 coefficients. The results for uncoded systems are depicted in Fig. 6. We compare both systems on the basis of the same bandwidth requirements and achievable data rate. In uncoded multicarrier systems the bit error ratio (BER) is generally dominated by bad subchannels, so that this does not privilege one of both systems.

The two solid black curves belong to CP-OFDM systems, where the lower is provided with the perfect instantaneous channel state information (CSI) and serves as a reference, whereas the other one has to cope with the pilot based channel estimation. Therefore, the difference indicates the performance loss due the estimation procedure.

The results show that increasing the number of equalizer coefficients from $N = 2$ to $N = 20$ in the FBMC case yields only a slight improvement in the BER over the whole simulated E_b/N_0 region. Obviously, the HIPERLAN/2 simulation environment is satisfied with a short equalizer length.

Moreover, the FBMC systems outperform OFDM in the high E_b/N_0 region due to the simpler modulation scheme. The FBMC curves are nearly identical $(N = 20)$ or slightly worse $(N = 2)$ in the low E_b/N_0 region. This effect is induced by the noisy channel estimation, which generates poor initial values for the LMS algorithm

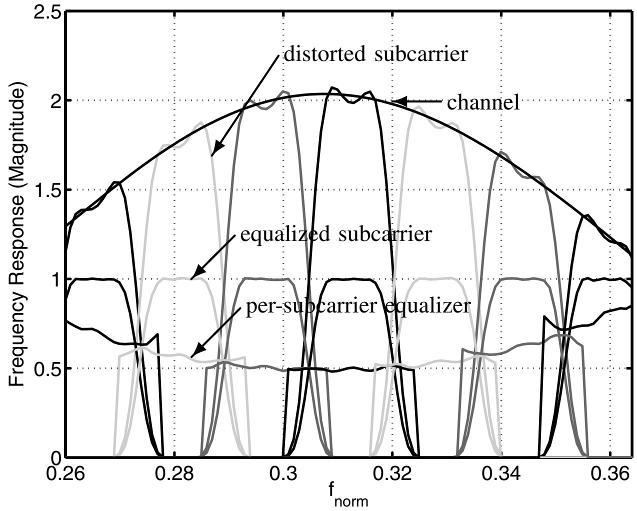

Fig. 7. Illustration of the Equalization of the Subchannels

and encumbers its convergence.

Fig. 7 illustrates the LMS equalization (noise-free) of the subchannels in the frequency domain, where the frequency axis is normalized with respect to the high sampling rate $1/(MT)$. The upper black contiguous curve is a section of the magnitude response of the frequency selective propagation channel covering 7 of the 52 used subchannels.

The subchannels are, therefore, distorted according to the channel characteristics. Each subchannel overlaps only with its directly adjacent subchannels. The 20-tap per-subchannel equalizers recover the Nyquist-shaped frequency responses from the distorted subchannels. This is crucial for the ISI and ICI elimination. It is also interesting to see that the frequency responses are almost flat in the passband region, which means that the per-subchannel equalizers also improved the frequency response of the shortly truncated RRC filters with $K = 4$ and a roll-off of $\rho = 0.5$.

The frequency responses of the subcarrier equalizers are as well depicted in Fig. 7 within the stopband edges of the corresponding subchannels. They complement each other to a curve which is approximately the inverse function of the channel magnitude response.

A. Comparison of Complexity

In the following we will define the term "flops" as number of real multiplications per symbol duration T. In order to get a notion of the computational complexity difference of the OFDM and FBMC system we calculate the number flops for both systems.

OFDM needs $2N_{\mathrm{FFT}}$ flops for the calculation of the IFFT and FFT at transmitter and receiver. There are additionally $4M_{\mathrm{t}}$ flops for the one-tap equalization at the receiver.

The FBMC system requires altogether $4N_{\mathrm{FFT}}$ flops for the IFFT and FFT operation at transmitter and receiver, if we use the regular MDFT structure of [8], because the IFFT/FFT operations are executed in $T/2$. It is worth mentioning, that this structure could in turn be optimized [7]. The polyphase filters contribute with further $8(MK+1)$ flops. The equalization takes place with $4NM_{\mathrm{t}}$ flops.

(9) combines these figures and yields the computational overhead μ of the FBMC system

$$\mu(N) = \frac{N_{\mathrm{FBMC}}(N)}{N_{\mathrm{OFDM}}} = \frac{N_{\mathrm{FFT}} + 2(MK+1) + NM_{\mathrm{t}}}{(1/2)N_{\mathrm{FFT}} + M_{\mathrm{t}}}. \quad (9)$$

If we use the split-radix algorithm which computes the M-point FFT/IFFT with $M(\log_2(M) - 3) + 4$ flops and the parameters of the simulation of Section V we get the following values $\mu(2) \approx 5$ and $\mu(20) \approx 10$. Due to the simplicity of the LMS algorithm the calculation of the complex valued equalizer coefficients (equalizer update) requires the same number $4NM_{\mathrm{t}}$ of flops as the application of the equalization itself.

VI. Conclusion

In this contribution we have modified the simple adaptive LMS algorithm to the requirements of OQAM-FBMCs. This modification can also be utilized for single-carrier systems with OQAM modulation. The LMS controlled per-subchannel equalizer operates as fractionally spaced $(T/2)$ equalizer in order to avoid irrevocable aliasing of the subchannels. We have compared its performance with a CP-OFDM system in a typical HIPERLAN/2 environment, where the difference in data rate has been compensated for by increasing the modulation scheme of OFDM from 16-QAM to 32-QAM. To have practical constraints the pilot symbols of HIPERLAN/2 have been used for CP-OFDM to get an estimation for its one-tap equalizer, whereas this estimation has been used as initial value for the LMS algorithm of the OQAM-FBMC.

The results show that the FBMC system with a simple LMS controlled equalizer already outperforms the CP-OFDM system in the medium to high E_{b}/N_0 region based on the same channel estimations. In the low E_{b}/N_0 region the results are very similar because the LMS algorithm suffers from a noisy initialization which encumbers its convergence.

Therefore, the additional computational complexity of the FBMC system, which benefits from the progress in integrated circuits, competes with many drawbacks of the CP-OFDM system like higher out-of-band emission, higher sensitivity to narrowband interferers, and a higher transmit power to achieve the same BER.

References

[1] T. Ihalainen *et. al.*, "Channel equalization in filter bank based multicarrier modulation for wireless communications," *EURASIP Journal on Advances in Signal Process.*, 2007.

[2] P. Siohan, C. Siclet, and N. Lacaille, "Analysis and design of OFDM/OQAM systems based on filterbank theory," *IEEE Transactions on Signal Processing*, vol. 50, no. 5, pp. 1170–1183, May 2002.

[3] ETSI TS 101 475 V1.3.1, "Broadband radio access networks (BRAN); HIPERLAN Type 2; physical (PHY) layer," 2001.

[4] L. G. Baltar, D. S. Waldhauser, and J. A. Nossek, "Out-of-band radiation in multicarrier systems: a comparison," in *Proc. MC-SS Workshop*. Springer, May 2007, pp. 107–116.

[5] B. Saltzberg, "Performance of an efficient parallel data transmission system," *IEEE Transactions on Communications*, vol. 15, no. 6, pp. 805–811, Dec. 1967.

[6] B. Hirosaki, "An orthogonally multiplexed QAM system using the discrete fourier transform," *IEEE Transactions on Communications*, vol. 29, no. 7, pp. 982–989, July 1981.

[7] T. Karp and N. J. Fliege, "Computationally efficient realization of MDFT filter banks," in *Proc. 8th European Signal Process. Conf.*, vol. 2, September 1996, pp. 1183–1186.

[8] ——, "Modified DFT filter banks with perfect reconstruction," *IEEE Transactions on Circuits and Systems—Part II: Analog and Digital Signal Processing*, vol. 46, no. 11, pp. 1404–1414, Nov. 1999.

[9] D. S. Waldhauser and J. A. Nossek, "MMSE equalization for bandwidth-efficient multicarrier systems," in *Proc. IEEE Int. Symp. Circuits Syst.*, 21-24 May 2006, pp. 5391–5394.

[10] S. Haykin, *Adaptive Filter Theory*, 4th ed. Prentice Hall, 2002.

[11] K.-D. Kammeyer, *Nachrichtenübertragung*, 3rd ed. Teubner, Nov. 2004.

[12] J. Medbo *et. al.*, "Channel models for HIPERLAN/2 in different indoor scenarios," *COST 259 TD (98) 70*, April 1998.